

JAAS

Accepted Manuscript



This is an *Accepted Manuscript*, which has been through the Royal Society of Chemistry peer review process and has been accepted for publication.

Accepted Manuscripts are published online shortly after acceptance, before technical editing, formatting and proof reading. Using this free service, authors can make their results available to the community, in citable form, before we publish the edited article. We will replace this *Accepted Manuscript* with the edited and formatted *Advance Article* as soon as it is available.

You can find more information about *Accepted Manuscripts* in the [Information for Authors](#).

Please note that technical editing may introduce minor changes to the text and/or graphics, which may alter content. The journal's standard [Terms & Conditions](#) and the [Ethical guidelines](#) still apply. In no event shall the Royal Society of Chemistry be held responsible for any errors or omissions in this *Accepted Manuscript* or any consequences arising from the use of any information it contains.

Determination of Ag, Cu, Mo and Pb in Soils and Ores by Laser-Induced Breakdown Spectrometry

Cite this: DOI: 10.1039/x0xx00000x

Andrey M. Popov*,^a Timur A. Labutin,^a Sergey M. Zaytsev,^a Irina V. Seliverstova,^a Nikita B. Zorov,^a Ildar A. Kalko,^b Yulia N. Sidorina,^b Ilya A. Bugaev^b and Yuriy N. Nikolaev^b

Received 00th January 2012,

Accepted 00th January 2012

DOI: 10.1039/x0xx00000x

www.rsc.org/

We report the results of analytical assessment of LIBS detection of silver, copper, lead and molybdenum in certified and natural soils and ores for the purposes of geochemical exploration. Strong matrix effects have been observed in case of molybdenum determination in soils and ores. Intensity of two Mo lines (313.26 nm and 550.65 nm) for ores was larger 3-5 times than for soils. We corrected such sample-to-sample variations by the proper selection of internal standard. There was no evidence of strong matrix effects in case of other elements. As typically happens in atomic emission spectroscopy, linear dynamic range of LIBS determination was narrow (1-100 ppm) for the resonance lines due to self-absorption. Detection limits of Ag, Mo, Cu and Pb were equal to 0.3 ppm, 0.3 ppm, 0.6 ppm and 8 ppm, respectively. Such sensitivity is sufficient to determine molybdenum, copper and lead at the level of their crustal abundance.

1. Introduction

Geochemical methods of prospecting are widely used in the all stages of a mineral exploration. More than 300 ore deposits were discovered with geochemical prospecting, including the biggest copper deposit Escondida, Chile (28.0 million tons).¹ The importance of geochemical data for environmental studies and analysis of natural background distribution of elements is also well established.² A few indispensable requirements have to be met for analytical methods to be sufficient for geochemical studies, namely the determination of the total amount of elements in the sample and the detection limits of all elements below their crustal abundances. The only combination of XRF spectrometry, ICP-AES, INAA, and, sometimes, element-specific techniques satisfies these requirements.³ The matter of developing suitable, sensitive and cost-effective analytical methods is therefore at the frontier of research. For some elements there is still a challenge of reducing the detection limits, so that they are one to two orders of magnitude below average concentrations in the various sample media.² Direct determination of the mineral composition based on Laser-Induced Breakdown Spectroscopy (LIBS) provide a unique opportunity to implement the principal requirement for the analysis of geochemical samples: sensitivity for a wide range of elements below their crustal abundances. It represents a rapid and low cost technique which can also be applied for the routine field activities. LIBS is a simple but highly versatile technique that allows detection a vast majority of chemical elements in any material – solid, liquid, or gas – at high

sensitivity with a single laser pulse.⁴ However, currently achieved detection limits amounting to dozens ppm for the main geochemical objects – soils, ores, rocks, and sediments are significantly above natural background.⁵ It is therefore highly beneficial to develop the methodological aspects of sensitivity enhancement of ore and soil analysis by the LIBS.

Since the elaboration of simultaneous LIBS determination of all 76 elements, recommended for geochemical prospecting, is hardly possible within a single paper, it seems reasonable to select a group of elements that are significant for the characterization of widespread ore bodies. Copper and polymetallic ores are among the most common objects of geochemical prospecting.⁶ The valuable markers for such ores are silver, copper, molybdenum and lead. Silver represents one of the challenging elements since its crustal abundance is 56 ppb.⁷ Ag concentration in ores and soils from most of silver deposits varies within 1-5 ppm and is considered to be geochemically anomalous.⁸ Copper abundance is 27 ppm.⁷ Usually ore samples from copper deposits contain more than 0.5 % wt. copper. In this case outline of copper anomalies in soils begins at about 100 ppm. Porphyry copper-molybdenum stockworks can be identified by soil anomalies of more than 500 ppm, while the content of 50 ppm is regarded as anomalous for gold-silver and silver-based polymetallic ores. Molybdenum is also the element of interest in geochemical prospecting because it often occurs together with copper (especially, the porphyry copper) and silver. Its background content is 0.8 ppm.⁷ Anomalous concentration in soils starts at 3-5 ppm, in

ores it reaches up to 0.1 % wt. of Mo. Abundance of lead is 11 ppm.⁷ Lead may be a valuable geochemical signature of porphyry copper objects since it concentrates in epithermal veins in porphyry systems⁹ and can be used to localize accompanying epithermal polymetallic mineralization.⁸ Also, prospective areas with gold-silver mineralization are usually framed by lead anomalies. A goal of our work was an assessment of figures-of-merit of LIBS technique as a tool for direct determination of important geochemical markers (Ag, Cu, Mo, and Pb) in ores and soils at the level close to their crustal abundances.

II. Experimental

(a) Experimental setup

The experimental setup was described in details elsewhere.¹⁰ We used the third harmonic at $\lambda=355$ nm of Nd:YAG laser (LOTIS TII, Belarus, 1-80 mJ/pulse, 8 ns, 5 Hz, beam diameter of 6 mm, divergence 0.8 mrad, ring-mode transverse structure), since it could provide a higher sensitivity than the fundamental and second harmonics.¹¹ The mirrors and achromatic doublet pair ($f = 150$ mm) focused a beam into the spot with diameter of 150 μm . Laser-induced plasma was projected by two-lens condenser ($f_1 = 100$ mm, $f_2 = 75$ mm) onto the slit of the high-aperture Czerny-Turner 0.32 m spectrograph HR-320 (ISA, USA) with decrease of an image 3:1. The narrow slit (25 μm) and the high density of a diffraction grating (1800 grooves/mm blazed at 200 nm) of spectrograph provided the high resolving power of ~ 8000 at 400 nm. The centre of the plasma plume, lenses and slit were aligned coaxially. ICCD camera "Nanogate-2V" (Nanoscan, Russia) was used to detect a spectral image of plasma radiation. We developed the special software in LabVIEW® environment to control the main parameters of camera (delay, gate, gain) and for the pre-processing of experimental spectra. This detector is also able to accumulate a signal from consequent laser pulses directly on CCD for low signal intensity, which gave the significant enhancement of the signal to noise ratio. We accumulated signal from 5 laser pulses for samples with analyte content below 15 ppm.

(b) Samples

In order to explore the feasibility of LIBS determination of Ag, Cu, Mo, and Pb, we studied overall 13 samples, which can be divided in four types. The first type represents the B horizon soils collected over the known mining trenches (Table 1, samples No.1-4). These samples allowed the delineation of the anomalous regions under the conditions of humid climatic zones. Based on the visual assessment, the soils were referred to tundra spodosol type with a low content of organic matter. Sampling of soil horizon was treated over the known ore intervals in the mining trenches. The quantitative analysis of soils was performed by means of ICP-AES After quartering, drying, grinding by a ball mill, and sieving (mesh ~ 70 μm). A 0.25 g sample was completely digested with a mixture of

Table 1. Composition of ores and soils used in this work.

N.	Description	Ag, ppm	Cu, ppm	Mo, ppm	Pb, ppm
1		4.1	4000	58	370
2	B horizon soils over the known ore bodies	0.7	6320	71	230
3		4.3	300	12	58
4		3.6	>10000	144	773
5		14.5	3260	3920	777
6	ore samples with porphyry molybdenum-copper mineralization	28.2	15500	72	170
7		36.9	2140	512	477
8		16.7	550	415	379
9	ore samples with silver-polymetallic mineralization	87	1290	4	537
10		15120	2364	2	20759
11		1570	4830	13	2704
12	ore samples with gold-silver mineralization	1300	23475	<1	2174
13		314	29	3	27
14	NIST 2709a	0.64	33.9 \pm 0.5	-	17.3 \pm 0.1
15	NIST 2710a	40	3420 \pm 50	-	5520 \pm 30
16	NIST 2711a	6	140 \pm 2	-	1400 \pm 10
17	BAM U110	4.51	263 \pm 12	2.5	197 \pm 14
18	Russian CRMs of red soil	0.06	47 \pm 2	3 \pm 1	23 \pm 4
19			170 \pm 20	8 \pm 3	150 \pm 30
20			310 \pm 10	13 \pm 2	280 \pm 60
21	Russian CRMs of gray calcareous soil	0.099	34 \pm 4	1.4 \pm 0.3	17 \pm 2
22			120 \pm 10	6 \pm 2	100 \pm 10
23			290 \pm 10	13 \pm 3	280 \pm 10
24	Russian CRMs of sandy podzolic soil	0.04	9 \pm 4	1.5 \pm 0.6	8 \pm 1

perchloric, nitric, hydrofluoric and hydrochloric acids in accordance the conventional technique ASY-4A01. The accuracy was estimated as to 1%. The results of the analysis are given in Table 1.

The rest three types of samples represent the ores originated from three potentially prospective deposits of the porphyry copper-molybdenum with associated gold (samples No.5-8 in Table 1), the silver-polymetallic (samples No.9-11 in Table 1) and the gold-silver (samples No.12-13 in Table 1). Ore from the gold-silver deposit No.1 (Kayenmyvaam, Russia) was quartz with sulphide mineralization (1-10 %). Gangue minerals were quartz with subordinate adularia and carbonate. Ore minerals included chalcopyrite, bornite, pyrite, gold and silver tellurides. Ore from the silver-polymetallic deposit No.2 (Uteveem, Russia) was also quartz with sulphide and supergene minerals of total amount less than 1 wt. %. Gangue minerals were quartz-adularia, chlorite, sericite, fluorite, cerussite; and ore minerals were galena, sphalerite, fahlite, acanthite, pyrite, chrysocolla, malachite, and native gold. Porphyry copper-molybdenum samples were collected from the Nakhodka ore field (Chukotka Peninsula, Russia). These samples were characterized by the quartz-sericite-feldspar composition. The content of ore minerals was about 1-5 % of the total sample mass, including molybdenite, chalcopyrite, pyrite, hessite, sphalerite, fahlite, galena and supergene minerals of copper, lead, molybdenum and iron. The determination of the element composition of ore samples was similar to the procedure for tundra spodosol soils (see Table 1).

A number of certified reference materials of soils (NIST, BAM, and Russian soils) were utilized (samples No.14-24 in Table 1). These soils represented several types of the most

widespread soils: sandy podzolic soils, red soils, grey calcareous soils, contaminated industrial and agricultural soils. It should be noted that Mo content in soils is usually low due to its crustal abundance. Therefore, molybdenum was not certified in several reference samples (NIST, samples No.14-16 in Table 1). Russian CRMs (samples No.18-24) contained silver at the background level. Reference materials represented powders with the size of grains below 63 μm (BAM), 74 μm (NIST), and 90 μm (Russian soils). Before analytical measurements, samples were pressed into a pellet with the diameter of 12 mm and the thickness of $\sim 2\text{-}3$ mm under a pressure of ~ 750 MPa.

III. Results and discussions

(a) Selection of analytical lines

In visible and near UV ranges, molybdenum has a number of lines belonging to three multiplets $y^7P^{\circ} \rightarrow a^7S$, $z^7P^{\circ} \rightarrow a^7S$ and $z^5P^{\circ} \rightarrow a^5S$ (see Table 2). To our best knowledge, there is no information about LIBS determination of Mo in soils or ores. Probable spectral interferences with lines of matrix components of soils and ores as well as the parameters of probable analytical lines are compared in Table 2. We considered lines of main components (iron, aluminium, calcium, magnesium, silicon) within an interval ± 0.1 nm around an analytical line as interfering ones. Parameters of lines were retrieved from NIST Atomic Database¹² and Kurucz Atomic Database¹³. The range of 380-390 nm seems to be inappropriate because of the considerable overlapping between the analytical lines of Mo I and the strongest lines of Fe I, while the Mo I lines within the range of 315-318 nm can be strongly disturbed by a number of the strong and broad Ca II lines. It was a reason to drop off Mo I 315.82 nm, Mo I 317.03 nm and Mo I 319.40 nm from a set of analytical lines. Since non-resonance lines of Mo I, interfering weakly with iron lines in the range of 550-560 nm, were used as analytical ones to quantify molybdenum in steels^{14,15} and fertilizers¹⁶ and our ICCD had high efficiency at this range, we examined three lines in this range. Moreover, the excitation potentials of these lines are less than those of Mo I 313.26 nm (see Table 2). LIBS spectra of three ores (samples No.5-7) in ranges of 313-320 nm and 549-558 nm are given in Figure 1,a and Figure 1,b, respectively. The temporal parameters for both ranges were delay of 2 μs and gate of 2 μs . Self-absorption of Mo I 313.26 nm is clearly visible for the sample No.5 with 3920 ppm of Mo. Strong line Ba I 553.55 nm is overlapped with Mo I 553.30 nm, therefore, this Mo I line seems to be unsuitable for the quantitative analysis.

The strongest lines of Ag I and Cu I belong to doublets $5^2P^{\circ} \rightarrow 5^2S$ and $4^2P^{\circ} \rightarrow 4^2S$, respectively. LIBS spectra of ore samples No. 8, 9, 12, obtained in the range of 323-339 nm at delay of 2.5 μs and gate of 2 μs , are shown in Figure 1,c. As one can see, Ag I 328.07 nm is rationed to Ag I 338.29 nm as 2:1 that is in a good agreement with the transition probabilities of these lines (see Table 2). We excluded Ag I 338.29 nm from the further consideration because of overlapping with a medium line of Fe I 338.39 nm and the loss of sensitivity for low

Table 2. Comparison of several lines of Mo, Cu, Ag, Pb and possible lines of main components of soils and ores interfering with analytical one.

Species	Multiplet	Lines, nm	$gA \times 10^7, \text{s}^{-1}$	E, eV	Interfering lines*
Mo I	$y^7P^{\circ} \rightarrow a^7S$	313.259	160.7	3.956	Fe I 313.25 w
		317.035	95.9	3.909	Fe II 317.03 w Ca II 317.93 vs
		319.398	76.6	3.881	Ca II 318.13 s Fe I 319.32 m
	$z^7D^{\circ} \rightarrow a^7S$	315.817	32.4	3.925	Fe I 315.79 w Ca II 315.89 vs
		379.825	62.1	3.263	Fe I 379.85 vs
		386.410	43.6	3.208	Fe I 386.38 m
	$z^7P^{\circ} \rightarrow a^7S$	390.295	30.8	3.176	Fe I 390.29 vs
		550.649	25.2	3.586	Fe II 550.62 m Fe I 550.68 m
		553.303	18.6	3.576	Ba I 553.55 s
	Ag I	$5^2P^{\circ} \rightarrow 5^2S$	557.044	9.9	3.560
328.068			56	3.778	Fe I 328.03 w Fe II 328.13 w
338.288			26	3.664	Fe I 338.24 w Fe I 338.39 m
Cu I	$4^2P^{\circ} \rightarrow 4^2S$	324.754	54.8	3.817	Fe I 324.70 w Fe I 324.72 w Fe I 324.82 w
		327.395	27.2	3.786	Ca I 327.46 m
		283.305	17.4	4.375	Fe I 283.24 m Fe II 283.31 w
Pb I	$7^3P^{\circ} \rightarrow 7^3P$	363.957	10.2	4.375	Fe I 364.04 m
		368.346	15	4.334	Fe I 368.31 m Fe I 368.41 m
		405.781	26.7	4.375	Fe I 405.73 w Fe I 405.82 w

* w – weak line, m – medium line, s – strong line, vs – very strong line

content of Ag. Although recently Liu *et al.*¹⁷ could not detect silver in soils at 23 ppm level by means of LIBS, the resonance line of Ag I 328.07 nm was visible for sample No.8 with 16 ppm of Ag even under non-optimal conditions. Cu I 324.75 nm seems to be more preferable for analytical purposes than line at 327.40 nm due to a twice higher transition probability and a possible disturbance of copper signal by the medium Ca I 327.46 nm line (see Table 2). It should be noted that Cu I 324.75 nm is strongly self-absorbed above 300 ppm.¹⁸ The lines from triplets $5^2D \rightarrow 5^2P^{\circ}$ (520.91 nm, 546.55 nm, 547.16 nm) and $4^2D \rightarrow 4^2P^{\circ}$ (515.32 nm, 521.82 nm, 522.01 nm) are usually explored to avoid self-absorption for samples with high content of silver and copper, respectively. These lines are likely to be less sensitive due to the high excitation potentials (about 6 eV), and we did not consider them as the analytical ones.

The strongest lead lines are the lines of multiplet $7^3P^{\circ} \rightarrow 7^3P$ presented in Table 2, therefore, they are usually served as the analytical lines for quantitative determination of lead by means of LIBS.^{18,19} Despite the spectral interferences from weak lines of iron, the most preferable line is Pb I 405.78 nm with respect to its transition probability and the spectral sensitivity of our ICCD. LIBS spectra of soil samples No.15-17 in the range of 402-409 nm are shown in Figure 1,d. The temporal parameters were 3.5 μs delay and 3 μs gate. Resuming, we examined two lines of Mo (313.26 nm and 550.65 nm) and three lines at 324.75 nm, 328.07 nm, and 405.78 nm of Cu, Ag, and Pb, respectively, to check LIBS feasibility of determination of the

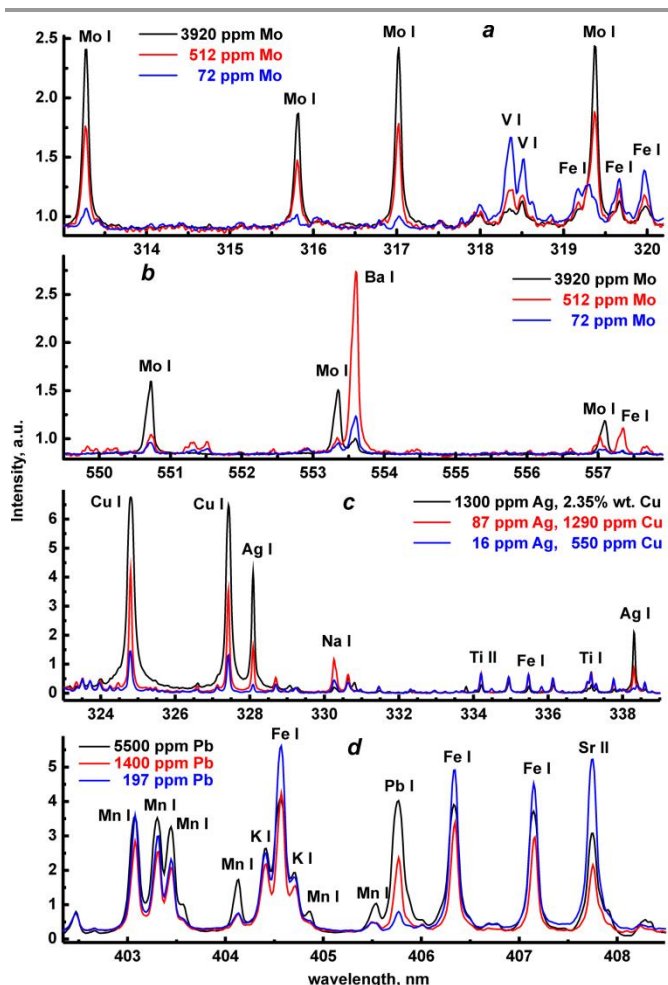


Figure 1. Emission spectra of several samples obtained within four spectral ranges: *a* 313–320 nm, *b* 549–558 nm, *c* 323–339 nm, *d* 402–408 nm. Content of elements of interest is given in a legend.

selected elements.

(b) Optimization of experimental parameters

We have studied the influence of experimental parameters on relative standard deviation (RSD) and the signal-to-noise ratio (SNR) to achieve the best experimental conditions in accordance with the recommendations of Tognoni *et al.*²⁰ A well-known fact is that the choice of the lens-to-sample distance (LTSD) limits the reproducibility of analytical measurements. For example, Popov *et al.*¹⁹ have demonstrated that the minimal value of RSD (~15 %) was achieved when the focus was 5 mm below the sample surface. They explained poor reproducibility (>150%) under exact focusing onto the surface as a result of pre-breakdown on the aerosol particles produced by the previous pulses. We observed similar behaviour of RSD of Ag line (curve 2 in Figure 2,a), which was calculated for 20 spectra (four pulse-to-pulse measurements in five points) of the ore sample No.9. Minimal RSD of Ag I line intensity was about 30% when the LTSD was 146 mm at the energy of 21 mJ (i.e. focal point was 4 mm below the sample surface). Moreover, the intensity of Ag line achieved maximal value near 146–148 mm (curve 1 in Figure 2,a) that was in the

agreement with the results obtained by Multari *et al.*²¹ for spherical lenses. They related such an effect to the higher plasma temperature under focusing a beam below 4–12 mm the sample surface. Therefore, for further measurements we have set LTSD of 146 mm.

Another important experimental parameter is a value of energy per pulse. In our studies, we varied the energy of laser pulse by a set of neutral filters. An influence of laser energy on RSD and the intensity of Ag line is shown in Figure 2,b. The intensity of Ag line grew with an increase of energy/pulse (curve 1 in Figure 2,b) due to larger mass ablated. The dependence of RSD on energy, as opposite to intensity, had a minimum at 18–21 mJ/pulse (curve 2 in Figure 2,b). Worsening RSD (up to 50% and more) at low energy can be a result of a proximity to the ablation threshold. The observed increase of RSD at high laser energies seems to be a result of random breakdown on the aerosol particles under the focusing conditions. For further measurements, we have chosen LTSD of 146 mm and energy of 21 mJ/pulse to find a compromise between maximal intensity and minimal RSD. Laser fluence under optimal conditions was ~120 J/cm².

(c) Heterogeneity effect

We have studied the heterogeneity of ores and soils sampled during geochemical prospecting in comparison with CRM. As an example of such a study, we used lead as an analyte in two

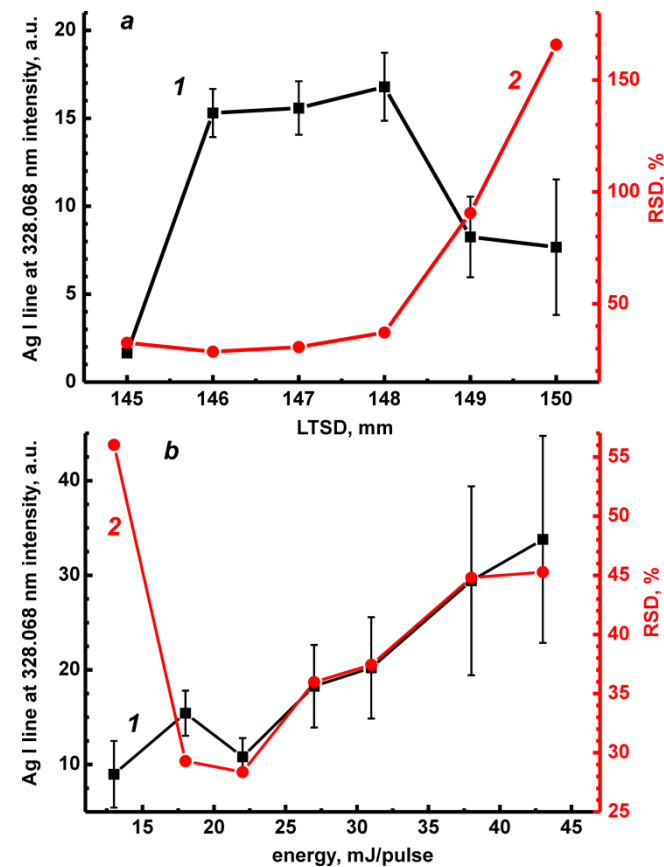


Figure 2. The intensity of Ag line (1, left axis) and its RSD (2, right axis) as a function of the lens-to-sample distance (*a*) and laser pulse energy (*b*).

soil samples: CRM of soil (sample No.23 with 280 ppm of Pb) and geochemical sample (sample No.2 with 230 ppm of Pb). We collected 10 pulse-to-pulse spectra in each of 10 randomly selected points on a surface. The pulse-to-pulse variations of Pb line at each point are shown in Figure 3 (curve 1, bottom part). Evident decreasing trend of lead signal seems to be due to the changes of focusing conditions. We suppose that RSD was varied between 30% and 100% from point to point mostly by two reasons. One of these reasons is the grain size distribution and its width (i.e. dispersion), since Sivakumar *et al.*²² have recently demonstrated the dependence of LIBS signal on particle size of the individual substance. Another possible reason is the variation of analyte content and its chemical form from grain to grain. Because the spot diameter (~150 μm) in our experiments was larger than maximal size of grains (90 μm for CRM of red soil), we suggested that grain size distribution could not strongly influence the RSD. Recently we have proposed²³ the use of Fe I line at 413.21 nm as an internal standard, based on the correlation criterion, to compensate for matrix effects on the Pb line. A trend of iron line shown in Figure 3 (curve 2, bottom part) was similar to the lead one. A ratio of these lines had quite different behavior (top part in Figure 3). Raw intensity of line was apparently inappropriate to make a decision on the outliers as well as the homogeneity of the sample. Unlike the raw intensity, the ratio obtained after internal standardization was virtually the same in 10 points of sample No.23, although there were several outliers in points 1, 7 and 10 (Figure 3). At the same time, the normalized lead signal in points 1 and 6 of sample No.2 was significantly different in comparison with other points. Perhaps, it was due to the enrichment of the sample with lead (e.g., which originated from the lead ore). We have used a set of values obtained at five consecutive pulses in 10 points randomly selected on the surface (i.e., 50 spectra) for averaging the heterogeneity of each sample. The described approach allowed the comparison of closeness between points in the set. Outliers, such as the point 1

of sample No.2 (Figure 3), were dropped from the set. Finally, the set consisted of 25-45 values.

(d) Analytical figures-of-merit

We have plotted the peak intensity of analytical line without a background as a function of the analyte content to assess the real possibility of LIBS for the quantitative determination of Ag, Cu, Mo and Pb in soils and ores. Examples of such dependencies are given in Figure 4. There were the considerable matrix effects for molybdenum, as a strong deviation of the dependencies between two types of matrixes (see the inset in Figures 4,e and 4,g). We have not observed such a deviation for Pb I 405.78 nm (Figure 4,c) as opposed to Eppler *et al.*²⁴ who have demonstrated strong matrix effects for Pb determination in soils. Moreover, there were no appreciable matrix effects for silver and copper (Figure 4,a and 4,b, respectively). Such an elemental peculiarity of matrix effects seems to be a result of the distinction between the chemical forms of molybdenum in ores and soils. Since the average content of Cu in soils is usually larger than 20-30 ppm, we prepared a sample with the lowest content of this analyte. For this purpose, a mixture of pure silica (as a main component of soils) and sample No.24 in weight ratio 1:1 was ground in an agate mortar into a dispersible fine powder. Resonance lines of copper and molybdenum were self-absorbed above 100 ppm (Figure 4,b and 4,e, respectively) that well agreed with a data on copper obtained by Hilbk-Kortenbruck *et al.*¹⁸

We selected an internal standard in accordance with the correlation criterion described earlier by us²³ to compensate for matrix effects. Let us remind a reader that the Fe I 413.21 nm was the reference line for Pb I 405.78 nm. For the other analytical lines, we have plotted the correlation spectra. Each spectrum represents a correlation coefficient between the intensity of analytical line and the intensity of any other pixel in the spectrum as a function of wavelength. We suggested that the lines, strongly correlated between each other ($R^2 > 0.8$), could be appropriate homologous pair. Unfortunately, in the

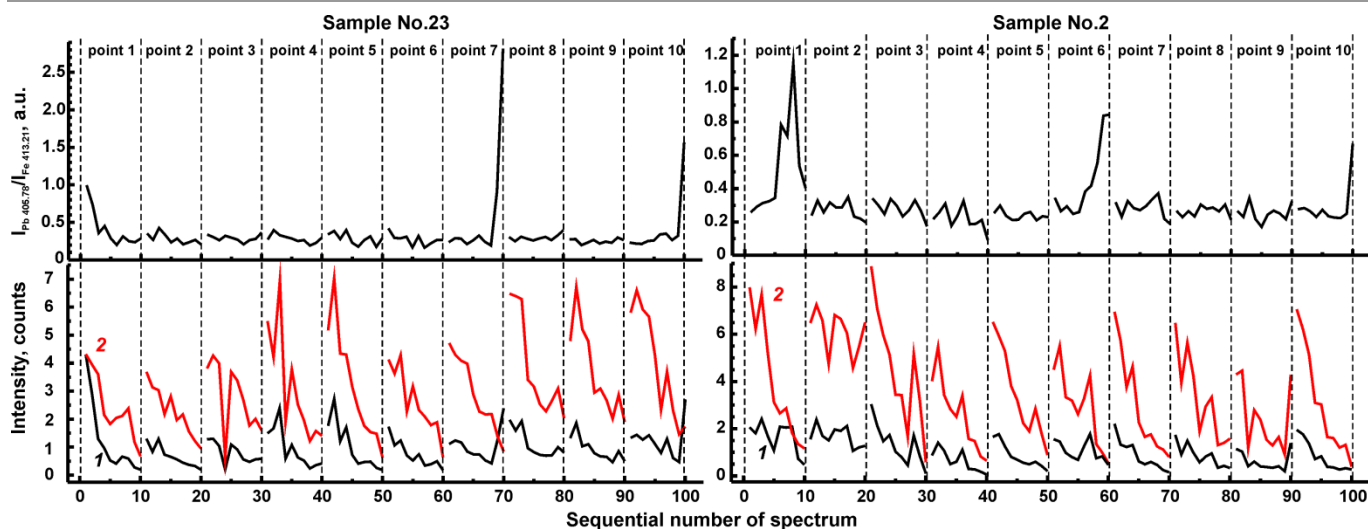


Figure 3. Pulse-to-pulse changes of Pb line (1, bottom), Fe line (2, bottom) and their ratio (top) for two samples in different points.

range 312–332 nm we did not observe any lines of the main components (Al, Fe, and Si) correlating strongly with the analytical one (the maximal value of R^2 was less than 0.6). Despite the presence of a number of Fe I lines with close excitation potentials within the range (e.g., Fe I 319.32 nm with $E=3.88$ eV), a linearity of the normalized calibration curves was dramatically worsened. Since there was no an appropriate homologous pair for copper and silver, we did not perform the internal standardization for these analytes. Moreover, the raw calibrations had a good linearity below 100 ppm (Figure 4,a and Figure 4,b). Fe I 313.41 nm had the best correlation with Mo I 313.26 nm ($R^2=0.85$), while Fe I 551.56 nm had the best correlation with Mo I 550.65 nm ($R^2=0.89$). Therefore, we have

chosen these iron lines as the internal standards for Mo analytical lines.

Parameters of the linear calibrations (slope, intercept, the correlation coefficient) obtained by some calibration methods are collected in Table 3. When a calibration function could not be approximated by a linear function in the whole range of contents (e.g., for Mo in Figure 4,f), we used the linear calibration within a narrower range of concentrations indicated in the last column of Table 3. Nevertheless, in such cases the calibration function was approximated by the Scheibe-Lomakin equation $y=a \times c^b$ in the whole range of contents. Such non-linear functions are also shown in Figure 4. The lowest content of analyte, for which the analytical line was clearly visible, was a lower limit of the linear dynamic range (LDR), while

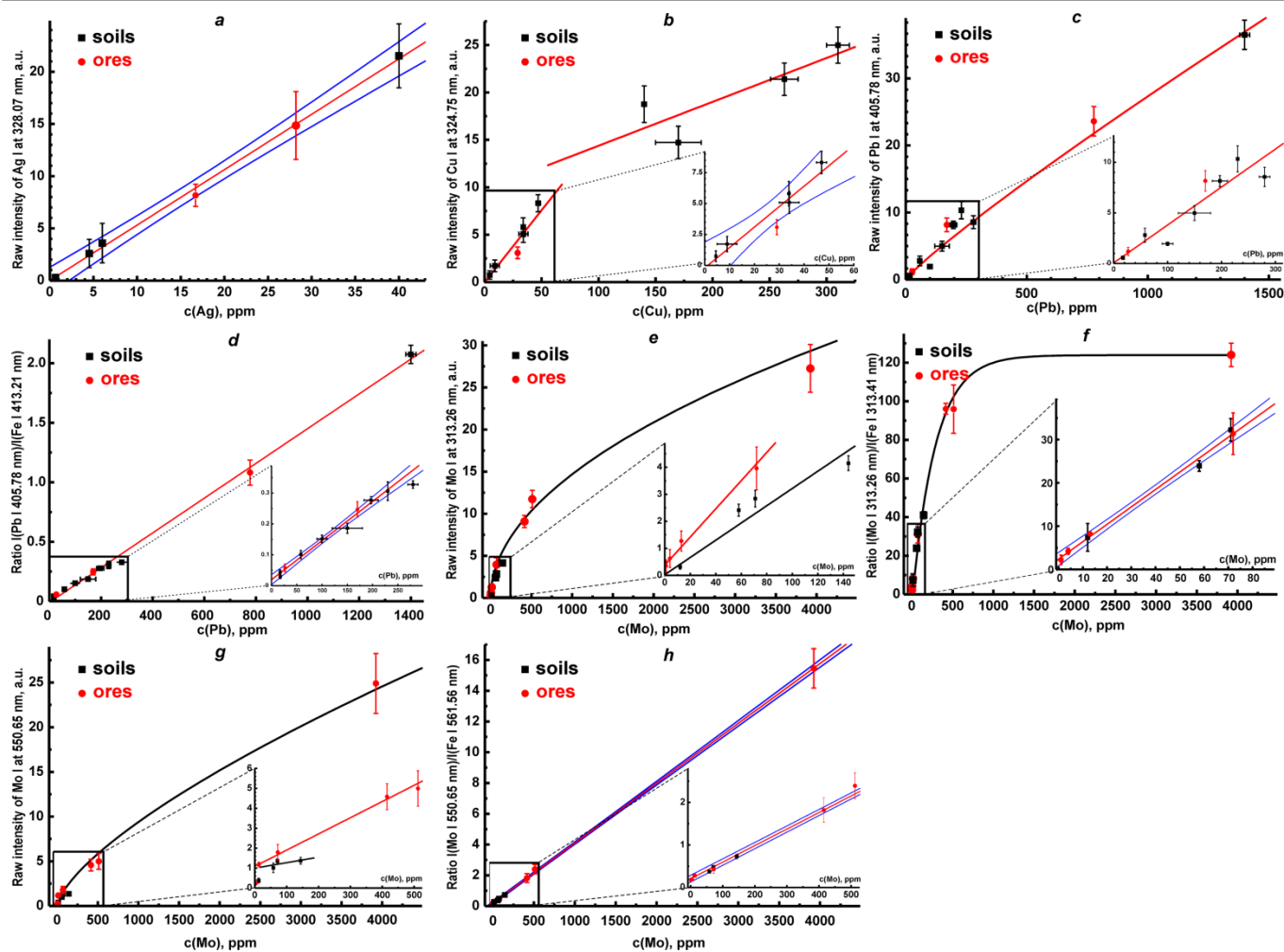


Figure 4. Raw intensities of lines of Ag I (a), Cu I (b), Pb I (c), Mo I (e,g), and the normalized intensities of Pb line (d) and Mo lines (f, h) as a function of the analyte content. The parts of function at low content of analytes are given in the insets as well as their linear approximations. Blue borders mark the confidence limits at the level of confidence probability of $P=0.99$.

a content of analyte at which calibration changed its slope due to self-absorption was an upper limit of LDR. An exception was silver for which the upper limit of LDR was established as a content in sample No.15. LDRs were narrower for resonance lines of Ag I 328.08 nm, Cu I 324.76 nm, and Mo I 313.26 nm, at least, by an order of magnitude than those for non-resonance lines of Pb I 405.78 nm and Mo I 550.65 nm. However, sensitivity of non-resonance lines was worse than for resonance lines, as it has been expected. Internal standardization for Pb and Mo lines allowed the significant enhancement of the calibration linearity and the reduction of strong matrix effects for molybdenum. A pronounced plateau in Figure 4,f probably resulted from that the line of Mo I 313.26 nm was widened above 500 ppm due to self-absorption and virtually merged with the small line of Fe I 313.41 nm (see Figure 1,a for 3900 ppm of Mo). Since we used the background corrected peak intensity as the line intensity, the intensity of Fe I line tended to the value of a point on the wing of molybdenum line with an increase of Mo content. Such an effect resulted in constant value of the ratio of Mo line to Fe line at high Mo content. Nevertheless, these lines were well resolved for low contents of molybdenum (see Figure 5,c); therefore, Fe I line can be used as the internal standard.

To illustrate the figures of merit of the developed technique for determination of Ag, Cu, Mo, and Pb, limits of detection (LODs) were calculated by 3σ -criterion: $\text{LOD} = 3\sigma_{\text{back}}/b$, where σ_{back} was a standard deviation of background (noises) and b was the slope of calibration curve. A value of σ_{back} was calculated as the noise nearby the analytical line for sample with the lowest content of analyte for the raw intensity. For normalized intensities, each point in the spectrum of sample with the lowest content of analyte after subtraction of a background line was normalized by the peak intensity of the reference line. The noise nearby the analytical line in normalized spectra was taken

as σ_{back} . LODs calculated through the different calibration methods are given in Table 3. Note that we did not calculate LOD for Mo I 550.65 nm in soils because of a poor quality of the calibration on raw spectra ($r^2=0.401$). It was probably due to the small interference lines: Fe II 550.62 nm and Fe I 550.68 nm. These strong matrix effects were observed for soils only (see the inset in Figure 4,g).

LOD of silver in the present work was 0.3 ppm, i.e. it was better by two orders of magnitude than achieved recently by Liu *et al.*¹⁷ by the combination of microwave excitation with laser ablation. A part of emission spectrum nearby Ag I line with the width of ~ 1 nm is demonstrated in Figure 5,a for sample No.17 (4.51 ppm Ag). One can see that Ag I line was between two strong lines of copper and iron. Unassigned lines can be resulted from the spectral interferences, especially, at the low content of silver. The resolution power should be improved for highlighting weak Ag I line with respect to the nearest strong lines to achieve the level of silver at its crustal abundance. We improved the LOD of copper determination in soils and ores with the use of the resonance lines by an order of magnitude than a level of 3-4 ppm achieved earlier.^{18,21} The use of non-resonance lines of copper with high excitation potentials had a low sensitivity. Therefore, LOD obtained by Dell'Aglio *et al.*²⁵ for Cu I 282.43 nm (5.7 eV) was 61 ppm, while LOD obtained by Bolger²⁶ for Cu I 330.79 nm (8.8 eV) was 300 ppm. Note, the multiline calibration used by Wisbrun *et al.*²⁷ allowed the decrease of LOD down to 20 ppm. The emission spectrum of sample No.24 after its dilution into two times (4.5 ppm of Cu) is shown in Figure 5,b. Weak lines of titanium and iron are probably limited the sensitivity of Cu I 324.75 nm line. We believe that the increase in sensitivity seems to have been achieved mainly by three reasons: (i) the use of third harmonic with the transverse mode stable from pulse to pulse; (ii) the projection of a laser plasma image on the entrance slit with a

Table 3. Analytical figures of merit of LIBS determination of Ag, Cu, Mo, and Pb in soils and ores obtained in the present work

Element	Analytical line, nm	LOD, ppm	Calibration method ^a	Parameters of linear regression			Linear dynamic range, ppm
				intercept	slope	r^2	
Ag	Ag I 328.08	0.3	Raw intensity (soil & ore)	650±200	(530±12)×10 ³	0.998	4.5-40
Cu	Cu I 324.75	0.6	Raw intensity (soil & ore)	200±500	1500±200	0.887	4.5-80
Pb	Pb I 405.78	8	IS Fe I 413.21 nm (soil & ore)	(19±7)×10 ⁻³	(127±3)×10 ⁻⁵	0.988	27-1500
		45	Raw intensity (soil & ore)	(4±73)×10 ⁴	3800±500	0.887	100-400
Mo	Mo I 313.26	0.3	IS Fe I 313.41 nm (soil & ore)	0.24±0.06	(40±1)×10 ⁻³	0.994	4-150
		3	Raw intensity (ore only)	(37±9)×10 ³	(52±6)×10 ²	0.964	12-200
		15	Raw intensity (soil only)	(2±20)×10 ⁴	(32±5)×10 ²	0.926	>58
	2.5	IS Fe I 561.56 nm (soil & ore)	0.21±0.02	(389±5)×10 ⁻⁵	0.999	12-4000	
	Mo I 550.65	10	Raw intensity (ore only)	(109±4)×10 ³	800±40	0.993	58-500
		-	Raw intensity (soil only)	(9±3)×10 ⁴	280±320	0.401	>144

^a IS denotes internal standardization of analytical line by reference one.

decrease compression; (iii) the accumulation of signal directly on the CCD for samples with a low content of copper and silver.

Although an excitation potential of Mo I 550.65 nm is 0.4 eV less than that of Mo I 313.26 nm (see Table 2), the sensitivity of Mo determination by means of line at 313 nm was better, at least, by an order of magnitude. We attributed this to overlapping of Mo I 550.65 nm, Fe II 550.62 nm and Fe I 550.67 nm (see Figure 5,d) in contrast to a line at 313 nm. We mentioned in Table 2 Fe I 313.25 nm as a possible interferent for Mo I 313.26 nm. One can obtain that the Fe I 313.41 nm is larger in 10 times than Fe I 313.25 nm following NIST database.¹² Since the intensity of the former iron line in Figure 5,c was smaller in ~4 times than Mo I 313.26 nm, a contribution of the latter iron line to the Mo line was less than 0.1. Therefore, we labeled molybdenum line as “Mo I + Fe I” in Figure 5,c. Emission spectra of sample No.14 and 16 containing

4 and 13 ppm of molybdenum are compared in Figure 5,c and 5,d, respectively. LOD of lead was 8 ppm, and it was similar to the results of Multari *et al.*²¹ and the field determination of lead above 10 ppm performed by Theriault *et al.*²⁸ The sensitivity of the determination on other lead lines was dramatically worse. For example, LOD for resonance line of Pb I 283.31 nm was 90 ppm¹⁹ while ion lines allowed the determination of lead above 45 ppm.²⁹ Emission spectrum of ore sample No.18 (27 ppm Pb) is demonstrated in Figure 5,e. One can see that the spectral interferences from the neighbouring lines limited the sensitivity: the variations of strong iron line at 406.21 nm caused evident changes in the background line of lead. RSD of analytical signal for low content of Ag, Cu, Mo and Pb did not exceed 20-25% as it can be seen from raw emission spectra demonstrated in Figure 5. After internal standardization, RSD was reduced up to 10%.

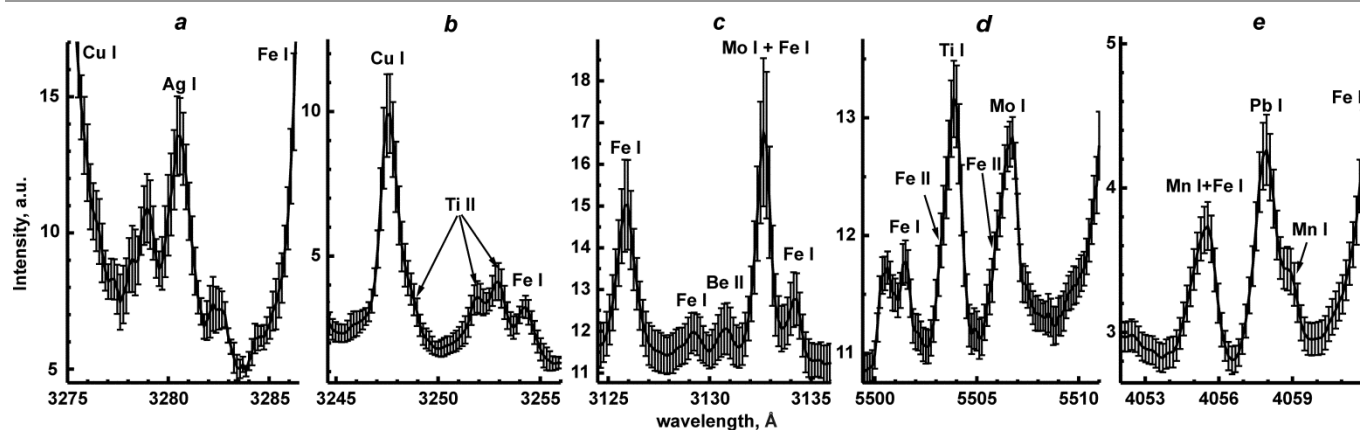


Figure 5. Emission spectra collected for the samples with the minimal content of analytes: 4.5 ppm Ag (a), 4.5 ppm Cu (b), 4 ppm Mo (c), 13 ppm Mo (d) and 27 ppm Pb (e). Bars indicate the standard deviation calculated for each point of averaged spectrum.

IV. Conclusions

LIBS is suitable for the quantitative determination of copper, lead and molybdenum in soils and ores at the levels of their crustal abundances. Therefore, the reliable and precise mapping for Cu, Pb, and Mo Mo, Pb, and Cu can be performed with LIBS during geochemical prospecting. Sensitivity of silver determination remains at the order of magnitude level worse than its background value. Nevertheless, there is the feasibility of LIBS to contour silver-ore/gold-ore deposits containing the increased Ag content due to large content of silver at such deposits. The larger resolution power and the aperture ratio of the spectrograph seem to be necessary for the decrease of LOD of silver. The use of double-pulse LIBS as an alternative way is questionable for LOD reduction, because Ag I 328.08 nm has a low excitation potential. On the other hand, the sensitivity achieved in the present work is dramatically better than the one of the direct determination of such elements by XRF spectrometry. The compact XRF analyzers allow the evaluation

of Ag, Cu, Mo, and Pb content with a high level of reliability as well as concentrations of other trace elements. The detection limits depend on matrix, tube power and type of the detector. Due to the common usage of the silver X-ray tubes, Ag content can be reliably identified in soils at the level of over 5 ppm, Cu – 50 ppm of, Mo – 15 ppm, Pb – 20 ppm.³⁰ These values correspond to the ones, obtained by portable XRF, which are about 10-30 ppm, 50 ppm, and 10-20 ppm, for silver, copper and lead respectively.³¹ LOD of molybdenum was about 10 ppm in geological samples by XRF used Mo K α (0.0709 nm).³² The strong spectral and matrix interferences are common for both XRF and LIBS analysis of soils and ores. However, we suppose that the selection of the delay and the gate and the increase of resolution power can reduce such influences. An important limitation of LIBS, as like as all emission techniques, is a narrow linear dynamic range (2-3 orders of magnitude) caused by self-absorption. In this case, we demonstrated that a suitable internal standard can slightly expand the range.

Acknowledgements

We thank Dr. Anastasia Drozdova for help in preparing the manuscript. We also thank Dr. Rob Lavinsky (iRocks.com) who kindly provided a photo of “Arkenstone specimen” for graphical abstract. This work was financially supported by Russian Scientific Foundation (grant No 14-13-01386).

Notes and references

^a Lomonosov Moscow State University, Department of Chemistry, Leninskie Gory, 1 bl.3, Moscow, 119991, Russia, e-mail: popov@laser.chem.msu.ru.

^b Lomonosov Moscow State University, Department of Geology, Leninskie Gory, 1, Moscow, 119991, Russia.

References

- 1 T. Brewis, *Min. Mag.*, 1990, 163, 173.
- 2 R.G. Garrett, C. Reimann, D.B. Smith, and X. Xie, *Geochem.-Explor. Environ. Anal.*, 2008, 8, 205.
- 3 X. Xie, *Analyst*, 1995, 120, 1497.
- 4 D.W. Hahn, and N. Omenetto, *Appl. Spectrosc.*, 2012, 66, 347.
- 5 R.S. Harmon, R.E. Russo, and R.R. Hark, *Spectrochim. Acta Part B*, 2013, 87, 11.
- 6 I.A. Baksheev, Y.N. Nikolaev, V.Y. Prokof'ev, E.V. Nagornaya, Y.N. Sidorina, L.I. Maruschenko, and I.A. Kal'ko, *Mineral deposit research for a high-tech world, Proceedings of 12th SGA Biennial Meeting 2013, Uppsala, Sweden*, 2, 766.
- 7 R.L. Rudnick, and S. Gao, *Composition of the Continental Crust/Treatise on Geochemistry*, 2003, 3, 1.
- 8 Y.N. Nikolaev, A.V. Apletalin, and I.A. Kal'ko, *Prospect and protection of mineral resources*, 2008, 4-5, 21.
- 9 R.H. Sillitoe, *Econ. Geol.*, 2010, 105, 3.
- 10 S.M. Zaytsev, A.M. Popov, N.B. Zorov, and T.A. Labutin, *J. Instrum.*, 2014, 9, P06010.
- 11 V. Piscitelli S., M.A. Martínez L., A.J. Fernández C., J.J. González, X.L. Mao, and R.E. Russo, *Spectrochim. Acta Part B*, 2009, 64, 147.
- 12 A. Kramida, Yu. Ralchenko, J. Reader and NIST ASD Team, *NIST Atomic Spectra Database (ver. 5.1) (2013) [Online]*. Available: <http://physics.nist.gov/asd> [2014, February 15].
- 13 1995, *Atomic Line Data* (R. L. Kurucz and B. Bell) Kurucz CDROM no. 23, Cambridge, Mass., Smithsonian Astrophysical Observatory, <http://www.cfa.harvard.edu/amp/ampdata/kurucz23/sekur.html>.
- 14 C.M. Davies, H.H. Telle, and A.W. Williams, *Fresenius J. Anal. Chem.*, 1996, 355, 895.
- 15 Z.N. Wang, Y. Li, Q.Y. Zhang, Y. Lu, and R.E. Zheng, *Spectrosc. Spect. Anal.*, 2011, 31, 1697.
- 16 W.A. Farooq, F.N. Al-Mutairi, A.E.M. Khater, A.S. Al-Dwayyan, M.S. AlSalhi, and M. Atif, *Opt. Spectrosc.*, 2012, 112, 874.
- 17 Y. Liu, B. Bousquet, M. Baudelet, and M. Richardson, *Spectrochim. Acta Part B*, 2012, 73, 89.
- 18 F. Hilbk-Kortenbruck, R. Noll, P. Wintjens, H. Falk, and C. Becker, *Spectrochim. Acta Part B*, 2001, 56, 933.
- 19 A.M. Popov, F. Colao, and R. Fantoni, *J. Anal. At. Spectrom.*, 2010, 25, 837.
- 20 E. Tognoni, V. Palleschi, M. Corsi, and G. Cristoforetti, *Spectrochim. Acta Part B*, 2002, 57, 1125.
- 21 R.A. Multari, L.E. Foster, D.A. Cremers, and M.J. Ferris, *Appl. Spectrosc.*, 1996, 50, 1483.
- 22 P. Sivakumar, L. Taleh, Y. Markushin, and N. Melikechi, *Spectrochim. Acta Part B*, 2014, 92, 84.
- 23 T.A. Labutin, S.M. Zaytsev, A.M. Popov, I.V. Seliverstova, S.E. Bozhenko, and N.B. Zorov, *Spectrochim. Acta Part B*, 2013, 87, 57.
- 24 A.S. Eppler, D.A. Cremers, D.D. Hickmott, M.J. Ferris, and A.C. Koskelo, *Appl. Spectrosc.*, 1996, 50, 1175.
- 25 M. Dell'Aglio, R. Gaudioso, G.S. Senesi, A. De Giacomo, C. Zaccone, T.M. Miano, and O. De Pascale, *J. Environ. Monit.*, 2011, 13, 1422.
- 26 J.A. Bolger, *Appl. Spectrosc.*, 2000, 54, 181.
- 27 R. Wisbrun, I. Schechter, R. Niessner, H. Schröder, and K.L. Kompa, *Anal. Chem.*, 1994, 66, 2964.
- 28 G.A. Theriault, S. Bodensteiner, and S.H. Lieberman, *Field Anal. Chem. Technology*, 1998, 2, 117.
- 29 S. Pandhija, and A.K. Rai, *Environ. Monit. Assess.*, 2009, 148, 437.
- 30 Y.N. Nikolaev, R.A. Mitoyan, Y.N. Sidorina, and T.N. Lubkova, *Prospect and protection of mineral resources*, 2013, 2, 52.
- 31 *Portable X-ray Fluorescence Spectrometry: Capabilities for in Situ Analysis*, ed. by P.J. Potts, M. West, 2008, RSC Publishing, 146.
- 32 A.K. Das, R. Chakraborty, M.L. Cervera, and M. de la Guardia, *Talanta*, 2007, 71, 987.